

## Late onset deficits in synaptic plasticity in the valproic acid rat model of autism

Henry Giles Stratten Martin and Olivier Manzoni

|                         |  |
|-------------------------|--|
| Journal Name:           | Frontiers in Cellular Neuroscience                           |
| ISSN:                   | 1662-5102  |
| Article type:           | Original Research Article                                    |
| First received on:      | 20 Dec 2013  |
| Revised on:             | 16 Jan 2014  |
| Frontiers website link: | <a href="http://www.frontiersin.org">www.frontiersin.org</a> |

1 **Late onset deficits in synaptic plasticity in the valproic acid rat model of**  
2 **autism**

3

4 **Henry G S Martin<sup>1,2,3</sup>, Olivier J Manzoni<sup>1,2,3\*</sup>**

5 <sup>1</sup>INSERM U901, Marseille, France

6 <sup>2</sup>INMED, Marseille, France

7 <sup>3</sup>Université de Aix-Marseille, UMR S901, Marseille, France

8

9

10

11

12 \* Correspondence:

13 Dr. Olivier Manzoni,

14 INSERM U901,

15 INMED,

16 Parc scientifique de Luminy

17 163 avenue de Luminy

18 13273 Marseille cedex 09

19 France

20 [olivier.manzoni@inserm.fr](mailto:olivier.manzoni@inserm.fr)

21

22

23

24 **Word Count: 3822**

25 **Number of Figures: 5**

26

27

28 **Keywords: Valproic acid, Prefrontal cortex, Synaptic plasticity, Autism, Age, NMDA receptor**

29

30 **Abstract**

31 Valproic acid (VPA) is a frequently used drug in the treatment of epilepsy, bipolar disorders and  
32 migraines; however it is also a potent teratogen. Prenatal exposure increases the risk of childhood  
33 malformations and can result in cognitive deficits. In rodents *in utero* exposure to VPA also causes  
34 neurodevelopmental abnormalities and is an important model of autism. In early postnatal life VPA  
35 exposed rat pups show changes in medial prefrontal cortex (mPFC) physiology and synaptic  
36 connectivity. Specifically, principal neurons show decreased excitability but increased local  
37 connectivity, coupled with an increase in long-term potentiation (LTP) due to an up-regulation of  
38 NMDA receptor (NMDAR) expression. However recent evidence suggests compensatory  
39 homeostatic mechanisms lead to normalization of synaptic NMDA receptors during later postnatal  
40 development. Here we have extended study of mPFC synaptic physiology into adulthood to better  
41 understand the longitudinal consequences of early developmental abnormalities in VPA exposed rats.  
42 Surprisingly in contrast to early postnatal life and adolescence, we find that adult VPA exposed rats  
43 show reduced synaptic function. Both NMDAR mediated currents and LTP are lower in adult VPA  
44 rats, although spontaneous activity and endocannabinoid dependent long-term depression are normal.  
45 We conclude that rather than correcting, synaptic abnormalities persist into adulthood in VPA  
46 exposed rats, although a quite different synaptic phenotype is present. This switch from hyper to  
47 hypo function in mPFC may be linked to some of the neurodevelopmental defects found in prenatal  
48 VPA exposure and autism spectrum disorders in general.

49

## 50 **1 Introduction**

51 Due to its anti-convulsant action and mood stabilizing properties valproic acid (VPA) is a common  
52 treatment for bipolar disorder and childhood epilepsy (McElroy et al., 1989). These stabilizing  
53 properties have been attributed to the action of VPA on GABA transaminobutyrate and sodium ion  
54 channels, however more recently VPA has been described as a histone deacetylase inhibitor  
55 (Göttlicher et al., 2001) leading to renewed interest in VPA for the treatment of a wide range of  
56 psychiatric and non-psychiatric diseases (Chateauvieux et al., 2010). Unfortunately VPA is also a  
57 potent teratogen and prenatal exposure increases the risk of congenital malformations and neural tube  
58 defects (Meador et al., 2008). Specifically VPA exposure *in utero* results in neurodevelopmental  
59 delays apparent in poor verbal performance and cognitive impairments (Nadebaum et al., 2011;  
60 Meador et al., 2013). Furthermore prenatal VPA exposure is associated with a seven-fold increased  
61 risk of developing autism spectrum disorders and is a significant prenatal hazard (Rasalam et al.,  
62 2005; Bromley et al., 2008; Christensen et al., 2013).

63 *In utero* injection of VPA during neural tube closure in rats and mice results in progeny that model  
64 some of the neurodevelopmental changes found in humans. Most prominent is an increase in autistic  
65 like behaviors in VPA exposed rodents; notably increased repetitive behaviors, reduced social  
66 interaction and hypersensitivity (Schneider and Przewłocki, 2004; Dufour-Rainfray et al., 2010;  
67 Gandal et al., 2010; Mehta et al., 2011; Kim et al., 2011). These behaviors have led to the proposal  
68 that *in utero* exposure to VPA may represent a useful rodent model of autism and is the basis of the  
69 “intense world theory” of autism (Markram et al., 2007).

70 Changes in local and distant connectivity in the brain has been proposed as a possible cause of  
71 autistic behavior (Geschwind and Levitt, 2007). Using the *in utero* VPA exposure model, local  
72 changes in principal neuron connectivity and excitability have been found in the rat medial prefrontal  
73 cortex (mPFC) (Rinaldi et al., 2008a, 2008b). This is perhaps particularly pertinent since the mPFC is  
74 linked to autistic behaviors and mPFC abnormalities are found in many neuropsychiatric disorders  
75 (Goto et al., 2010). The mPFC synaptic physiology in the VPA exposed rat pups appears to be tuned  
76 to a hyper-connected, hyper-excitabile state, notable for an increase in NMDA receptor (NMDAR)  
77 synaptic expression and an enhancement of long-term potentiation (LTP) (Rinaldi et al., 2007,  
78 2008b; Kim et al., 2013). However, recent recordings from older adolescent VPA exposed rats (P30  
79 days) have suggested a normalization of both synaptic physiology and neuronal excitability to naïve  
80 levels as pups develop (Walcott et al., 2011). In common with autism spectrum disorders, behavioral  
81 deficits are present throughout life in the rat VPA model (Rouillet et al., 2013), however a description  
82 of adult synaptic physiology is lacking making it unclear if the synaptic compensatory mechanisms  
83 found at P30 extend into adulthood.

84 In this study we have examined synaptic physiology in the mPFC of the prenatally VPA exposed rat  
85 from adolescence into adulthood. Surprisingly we find a reversal of the enhanced synaptic NMDAR  
86 expression phenotype found in VPA rat pups; such that adult VPA exposed neurons show a deficit in  
87 NMDAR mediated currents. Furthermore these adult neurons show a loss of LTP compared to  
88 controls, but unaltered long-term depression (LTD).

## 89 **2 Materials and methods**

### 90 **2.1 Animals**

91 All animals were group housed with 12 h light/dark cycles in compliance with the European  
92 Communities Council Directive (86/609/EEC). Time-mated female Wistar rats received a single  
93 intra-peritoneal dose of 600 mg/kg valproic acid (VPA, Sigma; prepared as 300 mg/ml saline  
94 solution) at gestational day E12 (Schneider and Przewlocki, 2004). Control dams received a single  
95 similar volume injection of saline at the same gestational time-point. Adolescent rats were  $P48 \pm 2$   
96 days (VPA: 3 males, 1 litter; Saline: 3 males, 1 litter); adult rats were  $P120 \pm 10$  days (VPA: 9 males,  
97 2 litters; Saline: 7 males, 2 litters).

## 98 **2.2 Slice preparation and electrophysiology**

99 After isoflurane anesthetization and decapitation, brains were sliced (300  $\mu\text{m}$ ) in the coronal plane in  
100 a sucrose-based solution (in mM: 87 NaCl, 75 sucrose, 25 glucose, 4 KCl, 2.1  $\text{MgCl}_2$ , 0.5  $\text{CaCl}_2$  18  
101  $\text{NaHCO}_3$  and 1.25  $\text{NaH}_2\text{PO}_4$ ). Slices were allowed to recover for 60 min at 32–35°C in artificial  
102 cerebrospinal fluid (aCSF; 126 NaCl, 2.5 KCl, 2.4  $\text{MgCl}_2$ , 1.2  $\text{CaCl}_2$ , 18  $\text{NaHCO}_3$ , 1.2  $\text{NaH}_2\text{PO}_4$  and  
103 11 glucose; equilibrated with 95%  $\text{O}_2$ /5%  $\text{CO}_2$ ) before transfer to the recording chamber.

104 Whole-cell patch-clamp and extra-cellular field recordings were made from layer V/VI pyramidal  
105 cells in coronal slices of prelimbic PFC (Lafourcade et al., 2007). For recording, slices were  
106 superfused (2 ml/min) with aCSF. All experiments were performed at 32–35 °C. The recording aCSF  
107 contained picrotoxin (100  $\mu\text{M}$ , Sigma) to block  $\text{GABA}_A$  receptors. To evoke synaptic currents, 150-  
108 200  $\mu\text{s}$  stimuli were delivered at 0.1Hz through an aCSF-filled glass electrode positioned dorsal-  
109 medial to the recording electrode in layer V (Figure 1A). Pyramidal neurons were visualized using an  
110 infrared microscope (BX-50, Olympus). Patch-clamp experiments were performed with electrodes  
111 filled with a cesium methane-sulfonate based solution (in mM; 143  $\text{CH}_3\text{O}_3\text{SCs}$ , 10 NaCl, 1  $\text{MgCl}_2$ , 1  
112 EGTA, 0.3  $\text{CaCl}_2$ , 2  $\text{Na}^{2+}$ -ATP, 0.3  $\text{Na}^+$ -GTP, 10 glucose buffered with 10 HEPES, pH 7.3,  
113 osmolarity 290 mOsm). Prior to break-through into the cell, pipette capacitance was compensated  
114 and the reference potential of the amplifier was adjusted to zero. Junction potentials were not  
115 corrected. Electrode resistance was 3-5 MOhm. If access resistance was greater than 20 MOhm or  
116 changed by >20% during the period of recording, the experiment was rejected. During recording  
117 holding currents, series resistance and membrane time constant ( $\tau$ ) were monitored. Only  
118 monosynaptic EPSCs were recorded with a latency of < 5ms. In extracellular field experiments, the  
119 recording pipette was filled with aCSF. The glutamatergic nature of the field excitatory postsynaptic  
120 potential (fEPSP) was confirmed at the end of the experiments using the ionotropic glutamate  
121 receptor antagonist 6,7-dinitroquinoxaline-2, 3-dione (DNQX, 20  $\mu\text{M}$ ; NIMH)

122 Input-output profiles were recorded for all fEPSP recordings. For time course experiments the  
123 stimulation intensity was that necessary give a response 40 – 60 % of the maximal. fEPSPs were  
124 recorded at 0.1 Hz. Using the same stimulation intensity as baseline, LTP was induced by a repeated  
125 (4 times, 10 s interval) theta burst stimulation (TBS; 4 100 Hz pulses repeated 5 times separated by  
126 200 ms). LTD was likewise induced by a steady 10 Hz stimulation for 10 minutes.

## 127 **2.3 Data acquisition and analysis**

128 Data was recorded on a MultiClamp700B (Axon Instruments), filtered at 2kHz, digitized (10kHz,  
129 DigiData 1440A, Axon Instrument), collected using Clampex 10.2 and analyzed using Clampfit 10.2  
130 (all from Molecular Device, Sunnyvale, USA). Analysis of both area and amplitude of fEPSPs and  
131 EPSCs was performed.

132 The magnitude of LTP and LTD was calculated 25 - 30 minutes after tetanus as percentage of  
133 baseline responses. To determine the AMPA/NMDA ratio, the AMPAR component amplitude was  
134 measured from EPSC at -70mV. The NMDAR component amplitude was determined 50ms after the  
135 peak AMPAR-evoked EPSC at +40mV, when the AMPAR component is over (Kasanetz and  
136 Manzoni, 2009). In a subset of experiments the AMPAR mediated current was inhibited with the  
137 selective antagonist 2,3-dihydroxy-6-nitro-7-sulfamoyl-benzo[f]quinoxaline-2,3-dione (NBQX, 10  
138  $\mu$ M; NIMH) to confirm the absence of an AMPAR contribution to the measured NMDAR  
139 component (Figure 1B). Spontaneous EPSCs were analyzed with Axograph X (Axograph). Statistical  
140 analysis of data was performed with GraphPad Prism (GraphPad Software Inc., La Jolla, CA) using  
141 tests indicated in the main text after Grubbs' outlier subtraction (99% confidence). All values are  
142 given as mean  $\pm$  standard error, n values represent individual animals and statistical significance was  
143 set at  $*p < 0.05$  and  $**p < 0.01$ .

### 144 3 Results

#### 145 3.1 Late onset deficits in synaptic currents are found in the mPFC of adult VPA exposed rats

146 Recently it has been reported that mPFC hyper-function found in juvenile rats exposed to the  
147 teratogen VPA is corrected in adolescent rats (Walcott et al., 2011). If such a strong compensatory  
148 mechanism exists during pup development, we asked if these modifications persist into adulthood.  
149 We focused on glutamatergic synapses of principal neurons in layer V/VI of the prelimbic region of  
150 the mPFC. These output neurons not only show a full range of synaptic plasticity throughout  
151 development into adulthood, but are also implicated in mPFC linked synaptopathologies (Lafourcade  
152 et al., 2011; Iafrati et al., 2013; Kasanetz et al., 2013).

153 We first verified, as reported by Walcott et al. that synaptic gain function is normalized in adolescent  
154 VPA exposed rats by recording evoked synaptic AMPAR and NMDAR currents and using the ratio  
155 of the two events as a measure of their modification. Neurons from adolescent rats exposed either to  
156 VPA or saline *in utero* reliably showed evoked EPSCs when voltage-clamped at both -70 mV  
157 (negative deflections) and +40 mV (positive deflections, Figure 2A). In the mPFC, at -70 mV fast  
158 inward EPSCs are principally AMPAR mediated, whereas at +40 mV a mixed AMPAR and  
159 NMDAR outward current is detected. Thus we calculated an index for the ratio AMPAR to NMDAR  
160 mediated currents (AMPA-NMDA ratio) by dividing the maximal amplitude of the response at -70  
161 mV (AMPA), by the +40 response amplitude at a predetermined time point after the fast AMPAR  
162 event had decayed to zero (NMDA). In agreement with Walcott et al. we find that this measure is  
163 broadly the same in both saline and VPA exposed neurons in adolescent rats (Figure 2B).

164 Given this compensatory rebalancing of synaptic function in adolescent rats, we asked if a similar  
165 effect is found in adult rats exposed to VPA *in utero*. At P120 strong EPSCs could be evoked from  
166 deep layer mPFC neurons clamped at -70 mV in both saline and VPA treated rats, however responses  
167 recorded at +40 mV were notably reduced in VPA neurons (Figure 2C). Repeating the same measure  
168 used in the adolescent rats, we calculated the AMPA-NMDA in our adult animals (Figure 2D).  
169 Surprisingly we found that in rats exposed to VPA *in utero* there was a significant increase in the  
170 AMPA-NMDA ratio compared to saline controls ( $p = 0.024$ ; Mann-Whitney U test). Notably saline  
171 treated adult rats had an AMPA-NMDA ratio similar to the value calculated for adolescents, whereas  
172 VPA treated rats had an elevated AMPA-NMDA ratio compared to both of these groups. Therefore  
173 in contrast to the reported reduction in AMPA-NMDA ratio found in mPFC of juvenile VPA exposed  
174 rats (Rinaldi et al., 2007, 2008a), we find an increase in this index in adulthood.

175 Anecdotally the increase in AMPA-NMDA ratio found in adult VPA neurons appeared to be due to a  
176 change in NMDAR mediated currents; however a change in this index can be linked to a number of  
177 other synaptic parameters. Therefore we further characterized some of the basic properties of these  
178 synapses. Taking a systematic approach, we first measured field EPSPs (fEPSP) from layer V/VI  
179 neurons to build input-output profiles in saline and VPA neurons. fEPSPs evoked by electrical  
180 stimulation in the same layer showed a similar profile in response to increasing stimulation intensity  
181 (Figure 3A). Furthermore input-output curves from saline and VPA exposed neurons were nearly  
182 identical. Therefore these synapses do not show and gross changes in excitability.

183 To further characterize these synapses, we measured quantal events by recording spontaneous EPSCs  
184 (sEPSC). Both saline control and VPA neurons showed robust spontaneous EPSCs in adulthood  
185 (Figure 3B). We used the cumulative distribution of the amplitude of events to gauge any differences  
186 between the two groups (Figure 3C). However both the distribution and the mean amplitude of  
187 spontaneous events were broadly the same in VPA exposed and saline control neurons. At resting  
188 membrane potential (-70 mV) these events are principally AMPAR mediated, therefore as previously  
189 reported in adolescent animals (Walcott et al., 2011), VPA exposure does not appear to strongly  
190 effect AMPAR currents. Likewise, we compared the frequency of sEPSC by comparing the  
191 cumulative distribution of the interval between events (Figure 3D). Both saline and VPA exposed  
192 neurons had a similar distribution and average interval between events. Therefore both presynaptic  
193 release and post synaptic AMPAR are similar in control and VPA exposed neurons in the mPFC.

### 194 **3.2 Adult VPA mPFC neurons have deficits in LTP, but not LTD**

195 In juvenile rats exposed to VPA, a decrease in AMPA-NMDA ratio was linked to increased LTP in  
196 the mPFC (Rinaldi et al., 2007). Since in adult VPA exposed rats we observe the opposite  
197 phenomenon, we asked if adult VPA rats might instead show reduced LTP. We recorded fEPSPs in  
198 layer V/VI and challenged slices with a short theta burst stimulation (TBS) LTP protocol; this  
199 induces a post-synaptic NMDAR dependent form of LTP (Iafrati et al., 2013). In saline controls a  
200 robust potentiation of fEPSPs was observed that was stable over the period of recording. In contrast  
201 in recordings from VPA exposed neurons, fEPSPs were smaller than saline controls (Figure 4A).  
202 Taking the fEPSP strength pre and post TBS we compared LTP in saline and VPA treated rats  
203 (Figure 4B). In control slices TBS induced a significant LTP ( $p = 0.012$ ; Paired t test), whereas in  
204 VPA slices there we did not detect a significant potentiation ( $p = 0.177$ ; Paired t test). Converting the  
205 post TBS fEPSP to a percent LTP, we plotted the cumulative distribution of the percent LTP in  
206 individual experiments. The distribution of VPA exposed neurons is left shifted compared to saline  
207 controls, indicating a reduction in LTP (Figure 4C). Therefore in contrast to juvenile VPA exposed  
208 neurons in the mPFC, adult neurons show a reduction in NMDAR mediated LTP.

209 To confirm this reduction in LTP is a specific phenomenon linked to our observed changes in  
210 AMPA-NMDA ratio, we tested another form of activity dependent plasticity that is independent of  
211 NMDARs in the mPFC. Endocannabinoid-dependent long-term depression (eCB-LTD) induced by  
212 steady 10 Hz stimulation, engages an mGluR5 mediated mechanism that requires retrograde 2-AG  
213 signaling to presynaptic CB<sub>1</sub> receptors (Lafourcade et al., 2007, 2011). Recording fEPSPs from  
214 mPFC deep layers, we induced eCB-LTD in saline and VPA *in utero* treated adult rats. Both groups  
215 showed an initial strong depression in fEPSP in response to 10 Hz stimulation that stabilized at  
216 approximately 80 % of the baseline response (Figure 5A). Again we compared the response pre and  
217 post eCB-LTD (Figure 5B). In both saline controls and VPA exposed neurons we saw a significant  
218 depression of fEPSP (Saline:  $p = 0.042$ ; VPA:  $p = 0.005$ ; Paired t test). Converting fEPSPs to percent

219 LTD we compared the amount of depression in the two groups. Unlike LTP, the distribution and  
220 strength of LTD was similar between control and VPA neurons (Figure 5C). Therefore eCB-LTD is  
221 unaffected in adult rats exposed to VPA *in utero*.

## 222 4 Discussion

223 In this study we have traced changes in mPFC synaptic physiology in the VPA rat from adolescence  
224 to adulthood. Juvenile rats exposed *in utero* to the teratogen VPA have a hyper-connected mPFC  
225 with enhanced NMDAR function (Rinaldi et al., 2007, 2008b). However recent evidence suggests  
226 that this phenotype is normalized as pups reach puberty (Walcott et al., 2011). Given the late  
227 maturation of the PFC, we wished to extend this synaptic description into adulthood to better  
228 understand the developmental consequences VPA exposure. Surprisingly in contrast to VPA rat pups  
229 and adolescents, we found evidence of synaptic hypo-function during adulthood.

230 Compared to controls, VPA neurons in the mPFC show a reduced and delayed increase in AMPA-  
231 NMDA ratio over early post-natal development (Rinaldi et al., 2007; Walcott et al., 2011). However  
232 by the time rats reach early adolescence (P30) this parameter is similar in both VPA and saline  
233 controls. In concord we find that at puberty (P40-50) that the AMPA-NMDA ratio is not significantly  
234 different between control and VPA rats in the mPFC. However, when we extended measurement of  
235 the AMPA-NMDA ratio into young adulthood (P110-130) we found a significant increase of this  
236 index in VPA rats, but not controls.

237 The AMPA-NMDA ratio is a strong measure of synaptic state, particularly the relative number of  
238 AMPARs and NMDARs in the post-synapse (Watt et al., 2000), however other synaptic variables  
239 may also be involved. Therefore to better interpret the unexpected increase in AMPA-NMDA ratio in  
240 adult VPA rats, we measured quantal mPFC activity. Focusing on AMPAR mediated events we  
241 recorded spontaneous EPSCs in layer V/VI neurons. We found that neither the average amplitude nor  
242 distribution of spontaneous events was different in VPA and saline controls, indicating that synaptic  
243 AMPAR are unchanged in these rats. Likewise we failed to observe any change in frequency of  
244 spontaneous events. Superficially this is inconsistent with the local hyper-connectivity reported in the  
245 mPFC of juvenile VPA rats (Rinaldi et al., 2008b). However our measurements of spontaneous  
246 activity do not distinguish between local and distant connections, thus a relative reduction in distant  
247 connectivity could account for this inconsistency (Geschwind and Levitt, 2007; Rinaldi et al.,  
248 2008b).

249 The simplest interpretation of our AMPA-NMDA ratio in light of unchanged spontaneous activity is  
250 that NMDAR currents are reduced in adult rats exposed to VPA *in utero*. In the young VPA rat,  
251 Rinaldi et al. (2007) directly linked a decrease in AMPA-NMDA ratio to an increase in expression of  
252 GluN2a and GluN2b and a subsequent increase in LTP. Our increase in AMPA-NMDA ratio in the  
253 adult VPA rat was suggestive that the opposite phenomenon might occur in these older animals.  
254 Indeed, when we challenged deep layer mPFC neurons with TBS LTP protocol there was a  
255 measurable loss in potentiation with VPA exposure compared to saline controls. A similar NMDAR  
256 linked loss of LTP is found in a number of mouse genetic models of autism (Ebert and Greenberg,  
257 2013; Jiang and Ehlers, 2013), suggesting the adult VPA rat shares similarities with these mice. We  
258 found no change in mGluR5 mediated eCB-LTD in these synapses, demonstrating that this deficit in  
259 LTP is not a general loss of synaptic gain function.

260 Fragile X syndrome (FXS) is a genetic disorder with a complex endophenotype that often includes  
261 autism linked behaviors (Cornish et al., 2008). Similar to our findings in VPA rats, FXS mice show a  
262 reduction in NMDAR expression in the mPFC and a loss of LTP (Zhao et al., 2005; Meredith et al.,  
263 2007; Krueger et al., 2011). Likewise in young FXS mice (2 – 3 weeks) mGluR5 mediated LTD is  
264 unaffected (Desai et al., 2006; Meredith et al., 2007), although in adult mice a deficit in coupling  
265 between mGluR5 activation and retrograde signaling appears to be responsible for a loss in eCB-  
266 LTD (Jung et al., 2012). Similar to the VPA rat, age and development linked deficits in synaptic  
267 physiology appear to be present in the FXS mouse, although differences in early postnatal life  
268 suggest these two models of autism are not directly comparable (Desai et al., 2006; Rinaldi et al.,  
269 2007).

270 The surprising finding in this study is that rats prenatally exposed to VPA pass from an enhanced  
271 LTP phenotype in early life to a LTP deficit phenotype in adulthood. Immediately before puberty and  
272 during adolescence NMDAR mPFC physiology appears similar to saline control suggesting that VPA  
273 neurons transition through a normal period between a hyper to hypo synaptic function. It has been  
274 proposed that homeostatic compensatory mechanisms may be responsible for the initial  
275 normalization of mPFC neuronal function in VPA rats (Walcott et al., 2011). How these  
276 compensatory synaptic scaling mechanisms work is unclear, however our results suggest that the  
277 action of normalizing hyper function in early life may subsequently lead to the loss of LTP in  
278 adulthood. Such a rebound effect may be due to the engagement of feedback loops that act over  
279 extended periods of development. It is also noteworthy that in our recordings we average across layer  
280 V/VI neuronal responses. This is significant since layer V principal neurons appear to belong to one  
281 of two subtypes with differing intrinsic properties and output projects (Dembrow et al., 2010; Lee et  
282 al., 2014). Regardless our results strongly argue for the importance of longitudinal studies when  
283 investigating early changes in synaptic physiology.

284 Prenatally treated VPA rats show behavioral deficits that share similarities with core autistic  
285 behaviors, in common with a small percentage of children that develop autism due to an exposure to  
286 VPA during pregnancy (Roulet et al., 2013). A validation of our observations would be to link  
287 autism associated behaviors in the VPA rat at specific ages with deficits in mPFC plasticity.  
288 Consistent with a delay in normalizing synaptic currents in early post-natal development, VPA rats  
289 and mice show a latency in nest-seeking behavior and bedding odor discrimination compared to  
290 control pups (Schneider and Przewłocki, 2004; Roulet et al., 2013), although these behaviors are not  
291 mPFC dependent. Deficits in social interaction are more clearly linked to abnormalities in mPFC  
292 function and these are consistently reported in the VPA rat (Roulet et al., 2013). However, from the  
293 earliest time points (pre-weaning, (Roulet et al., 2010)), into adolescence and adulthood social  
294 deficits are found in VPA exposed rats (Schneider and Przewłocki, 2004; Dufour-Rainfray et al.,  
295 2010; Kim et al., 2011). Therefore a direct link to social behavior and age dependent changes in  
296 NMDAR mediated LTP does not appear to be present. This of course does not exclude the  
297 importance of increased synaptic NMDAR and LTP in the formation of a locally hyper-connected  
298 state in the VPA rat pup (Rinaldi et al., 2008a, 2008b). Other longitudinal tests of mPFC linked  
299 behaviors have not yet been reported in the VPA rat, although an adulthood deficit in radial maze  
300 learning is present (Narita et al., 2010). Ultimately a systematic test of mPFC dependent behaviors  
301 from adolescence to adulthood will be necessary to identify the specific late-onset behavioral deficits  
302 which our findings allude to.

## 303 **5 Acknowledgments:**

304 This work was supported by INSERM and ANR “RescueMemo”. We thank members from the  
305 Manzoni and Chavis laboratories for discussions, the National Institute of Mental Health’s Chemical  
306 Synthesis and Drug Supply Program (Rockville, MD, USA) for providing DNQX, and Dr. R. Nardou  
307 and Dr. D. Ferrari from Neurochlore (www.neurochlore.fr) for providing the VPA-treated rats.

## 308 **6** References

309 Bromley, R. L., Mawer, G., Clayton-Smith, J., and Baker, G. A. (2008). Autism Spectrum Disorders  
310 Following in Utero Exposure to Antiepileptic Drugs. *Neurology* 71, 1923–1924.

311 Chateauvieux, S., Morceau, F., Dicato, M., and Diederich, M. (2010). Molecular and Therapeutic  
312 Potential and Toxicity of Valproic Acid. *J. Biomed. Biotechnol.* 2010, 1–18.

313 Christensen, J., Grønberg, T. K., Sørensen, M. J., Schendel, D., Parner, E. T., Pedersen, L. H., and  
314 Vestergaard, M. (2013). Prenatal valproate exposure and risk of autism spectrum disorders  
315 and childhood autism. *JAMA* 309, 1696–1703.

316 Cornish, K., Turk, J., and Hagerman, R. (2008). The fragile X continuum: new advances and  
317 perspectives. *J. Intellect. Disabil. Res.* 52, 469–482.

318 Dembrow, N. C., Chitwood, R. A., and Johnston, D. (2010). Projection-Specific Neuromodulation of  
319 Medial Prefrontal Cortex Neurons. *J. Neurosci.* 30, 16922–16937.

320 Desai, N. S., Casimiro, T. M., Gruber, S. M., and Vanderklish, P. W. (2006). Early Postnatal  
321 Plasticity in Neocortex of Fmr1 Knockout Mice. *J. Neurophysiol.* 96, 1734–1745.

322 Dufour-Rainfray, D., Vourc’h, P., Le Guisquet, A.-M., Garreau, L., Ternant, D., Bodard, S., Jaumain,  
323 E., Gulhan, Z., Belzung, C., Andres, C. R., et al. (2010). Behavior and serotonergic disorders  
324 in rats exposed prenatally to valproate: A model for autism. *Neurosci. Lett.* 470, 55–59.

325 Ebert, D. H., and Greenberg, M. E. (2013). Activity-dependent neuronal signalling and autism  
326 spectrum disorder. *Nature* 493, 327–337.

327 Gandal, M. J., Edgar, J. C., Ehrlichman, R. S., Mehta, M., Roberts, T. P. L., and Siegel, S. J. (2010).  
328 Validating  $\gamma$  Oscillations and Delayed Auditory Responses as Translational Biomarkers of  
329 Autism. *Biol. Psychiatry* 68, 1100–1106.

330 Geschwind, D. H., and Levitt, P. (2007). Autism spectrum disorders: developmental disconnection  
331 syndromes. *Curr. Opin. Neurobiol.* 17, 103–111.

332 Goto, Y., Yang, C. R., and Otani, S. (2010). Functional and Dysfunctional Synaptic Plasticity in  
333 Prefrontal Cortex: Roles in Psychiatric Disorders. *Biol. Psychiatry* 67, 199–207.

334 Göttlicher, M., Minucci, S., Zhu, P., Krämer, O. H., Schimpf, A., Giavara, S., Sleeman, J. P., Lo  
335 Coco, F., Nervi, C., Pelicci, P. G., et al. (2001). Valproic acid defines a novel class of HDAC  
336 inhibitors inducing differentiation of transformed cells. *EMBO J.* 20, 6969–6978.

- 337 Iafrafi, J., Orejarena, M. J., Lassalle, O., Bouamrane, L., and Chavis, P. (2013). Reelin, an  
338 extracellular matrix protein linked to early onset psychiatric diseases, drives postnatal  
339 development of the prefrontal cortex via GluN2B-NMDARs and the mTOR pathway. *Mol.*  
340 *Psychiatry*. Available at:  
341 <http://www.nature.com/gate2.inist.fr/mp/journal/vaop/ncurrent/full/mp201366a.html>  
342 [Accessed November 7, 2013].
- 343 Jiang, Y., and Ehlers, M. D. (2013). Modeling Autism by SHANK Gene Mutations in Mice. *Neuron*  
344 78, 8–27.
- 345 Jung, K.-M., Sepers, M., Henstridge, C. M., Lassalle, O., Neuhofer, D., Martin, H., Ginger, M.,  
346 Frick, A., DiPatrizio, N. V., Mackie, K., et al. (2012). Uncoupling of the endocannabinoid  
347 signalling complex in a mouse model of fragile X syndrome. *Nat. Commun.* 3, 1080.
- 348 Kasanetz, F., Lafourcade, M., Deroche-Gamonet, V., Revest, J.-M., Berson, N., Balado, E.,  
349 Fiancette, J.-F., Renault, P., Piazza, P.-V., and Manzoni, O. J. (2013). Prefrontal synaptic  
350 markers of cocaine addiction-like behavior in rats. *Mol. Psychiatry* 18, 729–737.
- 351 Kasanetz, F., and Manzoni, O. J. (2009). Maturation of excitatory synaptic transmission of the rat  
352 nucleus accumbens from juvenile to adult. *J. Neurophysiol.* 101, 2516–2527.
- 353 Kim, K. C., Kim, P., Go, H. S., Choi, C. S., Yang, S.-I., Cheong, J. H., Shin, C. Y., and Ko, K. H.  
354 (2011). The critical period of valproate exposure to induce autistic symptoms in Sprague–  
355 Dawley rats. *Toxicol. Lett.* 201, 137–142.
- 356 Kim, K. C., Lee, D.-K., Go, H. S., Kim, P., Choi, C. S., Kim, J.-W., Jeon, S. J., Song, M.-R., and  
357 Shin, C. Y. (2013). Pax6-Dependent Cortical Glutamatergic Neuronal Differentiation  
358 Regulates Autism-Like Behavior in Prenatally Valproic Acid-Exposed Rat Offspring. *Mol.*  
359 *Neurobiol.*
- 360 Krueger, D. D., Osterweil, E. K., Chen, S. P., Tye, L. D., and Bear, M. F. (2011). Cognitive  
361 dysfunction and prefrontal synaptic abnormalities in a mouse model of fragile X syndrome.  
362 *Proc. Natl. Acad. Sci. U. S. A.* 108, 2587–2592.
- 363 Lafourcade, M., Elezgarai, I., Mato, S., Bakiri, Y., Grandes, P., and Manzoni, O. J. (2007). Molecular  
364 Components and Functions of the Endocannabinoid System in Mouse Prefrontal Cortex.  
365 *PLoS ONE* 2, e709.
- 366 Lafourcade, M., Larrieu, T., Mato, S., Duffaud, A., Sepers, M., Matias, I., De Smedt-Peyrusse, V.,  
367 Labrousse, V. F., Bretillon, L., Matute, C., et al. (2011). Nutritional omega-3 deficiency  
368 abolishes endocannabinoid-mediated neuronal functions. *Nat. Neurosci.* 14, 345–350.
- 369 Lee, A. T., Gee, S. M., Vogt, D., Patel, T., Rubenstein, J. L., and Sohal, V. S. (2014). Pyramidal  
370 Neurons in Prefrontal Cortex Receive Subtype-Specific Forms of Excitation and Inhibition.  
371 *Neuron* 81, 61–68.
- 372 Markram, H., Rinaldi, T., and Markram, K. (2007). The Intense World Syndrome – an alternative  
373 hypothesis for autism. *Front. Neurosci.* 15, 77–96.

- 374 McElroy, S. L., Keck, P. E., Jr, Pope, H. G., Jr, and Hudson, J. I. (1989). Valproate in psychiatric  
375 disorders: literature review and clinical guidelines. *J. Clin. Psychiatry* 50 Suppl, 23–29.
- 376 Meador, K. J., Baker, G. A., Browning, N., Cohen, M. J., Bromley, R. L., Clayton-Smith, J.,  
377 Kalayjian, L. A., Kanner, A., Liporace, J. D., Pennell, P. B., et al. (2013). Fetal antiepileptic  
378 drug exposure and cognitive outcomes at age 6 years (NEAD study): a prospective  
379 observational study. *Lancet Neurol.* 12, 244–252.
- 380 Meador, K., Reynolds, M. W., Crean, S., Fahrbach, K., and Probst, C. (2008). Pregnancy outcomes  
381 in women with epilepsy: A systematic review and meta-analysis of published pregnancy  
382 registries and cohorts. *Epilepsy Res.* 81, 1–13.
- 383 Mehta, M. V., Gandal, M. J., and Siegel, S. J. (2011). mGluR5-Antagonist Mediated Reversal of  
384 Elevated Stereotyped, Repetitive Behaviors in the VPA Model of Autism. *PLoS ONE* 6,  
385 e26077.
- 386 Meredith, R. M., Holmgren, C. D., Weidum, M., Burnashev, N., and Mansvelder, H. D. (2007).  
387 Increased threshold for spike-timing-dependent plasticity is caused by unreliable calcium  
388 signaling in mice lacking fragile X gene FMR1. *Neuron* 54, 627–638.
- 389 Nadebaum, C., Anderson, V., Vajda, F., Reutens, D., Barton, S., and Wood, A. (2011). The  
390 Australian brain and cognition and antiepileptic drugs study: IQ in school-aged children  
391 exposed to sodium valproate and polytherapy. *J. Int. Neuropsychol. Soc. JINS* 17, 133–142.
- 392 Narita, M., Oyabu, A., Imura, Y., Kamada, N., Yokoyama, T., Tano, K., Uchida, A., and Narita, N.  
393 (2010). Nonexploratory movement and behavioral alterations in a thalidomide or valproic  
394 acid-induced autism model rat. *Neurosci. Res.* 66, 2–6.
- 395 Rasalam, A. D., Hailey, H., Williams, J. H. G., Moore, S. J., Turnpenny, P. D., Lloyd, D. J., and  
396 Dean, J. C. S. (2005). Characteristics of fetal anticonvulsant syndrome associated autistic  
397 disorder. *Dev. Med. Child Neurol.* 47, 551–555.
- 398 Rinaldi, T., Kulangara, K., Antonello, K., and Markram, H. (2007). Elevated NMDA receptor levels  
399 and enhanced postsynaptic long-term potentiation induced by prenatal exposure to valproic  
400 acid. *Proc. Natl. Acad. Sci.* 104, 13501–13506.
- 401 Rinaldi, T., Perrodin, C., and Markram, H. (2008a). Hyper-connectivity and hyper-plasticity in the  
402 medial prefrontal cortex in the valproic acid animal model of autism. *Front. Neural Circuits*  
403 2, 4.
- 404 Rinaldi, T., Silberberg, G., and Markram, H. (2008b). Hyperconnectivity of Local Neocortical  
405 Microcircuitry Induced by Prenatal Exposure to Valproic Acid. *Cereb. Cortex* 18, 763–770.
- 406 Rouillet, F. I., Lai, J. K. Y., and Foster, J. A. (2013). In utero exposure to valproic acid and autism —  
407 A current review of clinical and animal studies. *Neurotoxicol. Teratol.* 36, 47–56.

- 408 Roullet, F. I., Wollaston, L., deCatanzaro, D., and Foster, J. A. (2010). Behavioral and molecular  
409 changes in the mouse in response to prenatal exposure to the anti-epileptic drug valproic acid.  
410 *Neuroscience* 170, 514–522.
- 411 Schneider, T., and Przewłocki, R. (2004). Behavioral Alterations in Rats Prenatally Exposed to  
412 Valproic Acid: Animal Model of Autism. *Neuropsychopharmacology* 30, 80–89.
- 413 Walcott, E. C., Higgins, E. A., and Desai, N. S. (2011). Synaptic and Intrinsic Balancing during  
414 Postnatal Development in Rat Pups Exposed to Valproic Acid in Utero. *J. Neurosci.* 31,  
415 13097–13109.
- 416 Watt, A. J., van Rossum, M. C. W., MacLeod, K. M., Nelson, S. B., and Turrigiano, G. G. (2000).  
417 Activity Coregulates Quantal AMPA and NMDA Currents at Neocortical Synapses. *Neuron*  
418 26, 659–670.
- 419 Zhao, M.-G., Toyoda, H., Ko, S. W., Ding, H.-K., Wu, L.-J., and Zhuo, M. (2005). Deficits in trace  
420 fear memory and long-term potentiation in a mouse model for fragile X syndrome. *J.*  
421 *Neurosci.* 25, 7385–7392.
- 422

423 **7 Figure Legends**

424 **Figure 1. AMPA – NMDA ratio experimental design.** (A) Bright-field snapshot of coronal slice  
 425 detailing prelimbic mPFC division (x-axis medial – lateral; y-axis dorsal – ventral). Typical  
 426 positioning of stimulation electrode (S) and patch-clamp recording electrode (R) are indicated (scale  
 427 bar 100  $\mu\text{m}$ ). (B) Example traces from AMPA – NMDA ratio calculation. NMDAR mediated current  
 428 was taken as  $V_C +40$  mV value 50 ms after peak AMPAR mediated current measured at  $-70$  mV  
 429 (indicated by dashed line). NBQX insensitive current (green) and subtracted current (red) at  $V_C +40$   
 430 mV show that AMPAR mediated currents are close to zero at NMDAR current measurement point.

431 **Figure 2. AMPA - NMDA ratio is increased in adult but not adolescent VPA mPFC neurons.**  
 432 (A) Example EPSCs recorded from visually identified pyramidal neurons in layer V/VI mPFC from  
 433 adolescent rats (P45-49). Negative traces represent inward evoked currents from neurons patch-  
 434 clamped at  $-70$  mV, positive traces represent outward evoked currents from neurons patch-clamped at  
 435  $+40$  mV. Scale bar 50 ms, 100 pA. (B) Average AMPA/NMDA ratio from adolescent rats exposed to  
 436 saline or VPA *in utero*. (C) Similar evoked example EPSC traces from visually identified deep layer  
 437 pyramidal neurons from adult rats (P110-130). (D) Average AMPA/NMDA ratio from adult rats  
 438 exposed to saline or VPA *in utero*. Data points represent AMPA/NMDA ratio from individual  
 439 animals. Data shown as mean  $\pm$  s.e.m.;  $*p < 0.05$ .

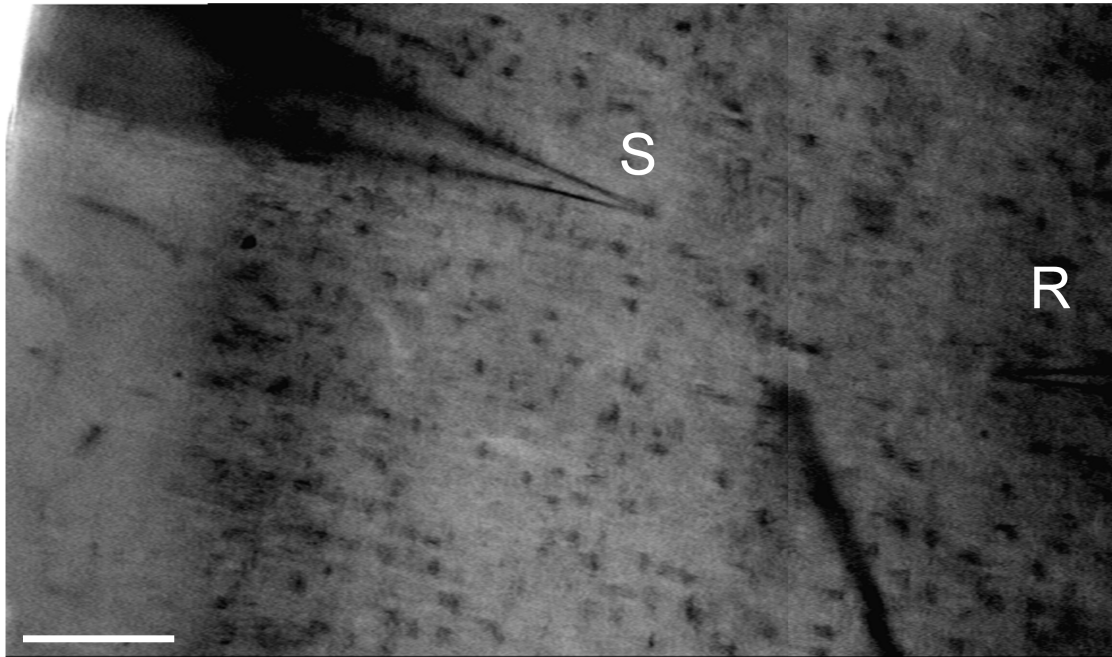
440 **Figure 3. Basal synaptic activity is normal in adult VPA neurons.** (A) Input – Output  
 441 relationships derived from evoked fEPSPs in deep layer mPFC. Sample fEPSP traces from saline and  
 442 VPA treated rats showing fEPSP change in response to 10 pA stimulation steps (top). Scale bar  
 443 10ms, 0.5 mV. Average fEPSP amplitude from saline and VPA neurons (bottom). (B) Spontaneous  
 444 EPSCs from pyramidal neurons patch-clamped at  $-70$  mV. Scale bar 0.5 s, 10 pA. (C) Cumulative  
 445 probability plot of individual spontaneous EPSCs from adult saline and VPA neurons. Average  
 446 amplitude EPSC from individual animals (insert; Saline,  $n = 5$ ; VPA,  $n = 7$ ). (D) Cumulative  
 447 probability plot of intervals between spontaneous EPSC events from saline and VPA neurons.  
 448 Average recorded interval between spontaneous events from individual neurons (insert). Data shown  
 449 as mean  $\pm$  s.e.m.

450 **Figure 4. Deficits in LTP are present in VPA exposed mPFC neurons.** (A) Time course of  
 451 normalized fEPSP responses from layer V/VI adult rats treated with saline or VPA *in utero*. Theta  
 452 burst LTP stimulation is indicated by arrow. (B) Change in normalized fEPSP pre- (Baseline) and  
 453 post- (LTP; 25 minutes after TBS) theta burst stimulation LTP. Darker points represent the mean  
 454 fEPSP. (C) Cumulative probability plot of percent LTP from individual experiments. Data shown as  
 455 mean  $\pm$  s.e.m.;  $**p < 0.01$ .

456 **Figure 5. LTD is normal in VPA exposed mPFC neurons.** (A) Time course of normalized fEPSP  
 457 responses from layer V/VI adult rats treated with saline or VPA *in utero*. 10 Hz eCB-LTD  
 458 stimulation is indicated by bar. (B) Change in normalized fEPSP pre- (Baseline) and post- (LTD; 25  
 459 minutes after 10 Hz stimulation) eCB-LTD. Darker points represent the mean fEPSP. (C)  
 460 Cumulative probability plot of percent LTD from individual experiments. Data shown as mean  $\pm$   
 461 s.e.m.;  $*p < 0.05$ ,  $**p < 0.01$ .

Figure 1.TIF

**A**



**B**

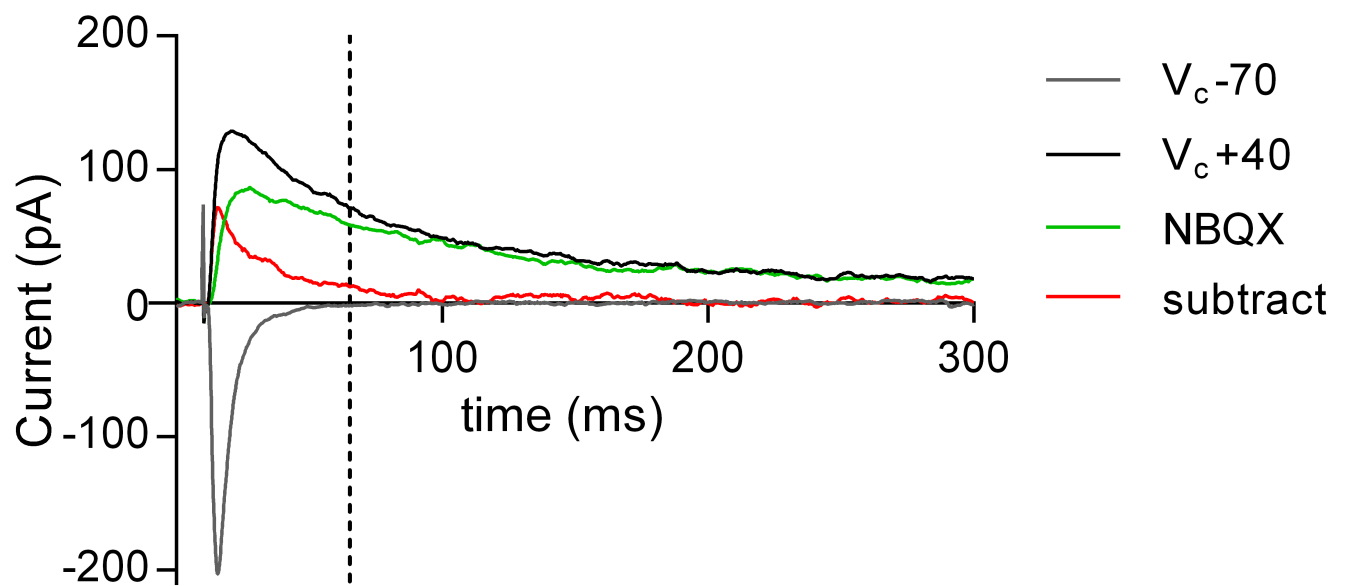


Figure 2.TIF

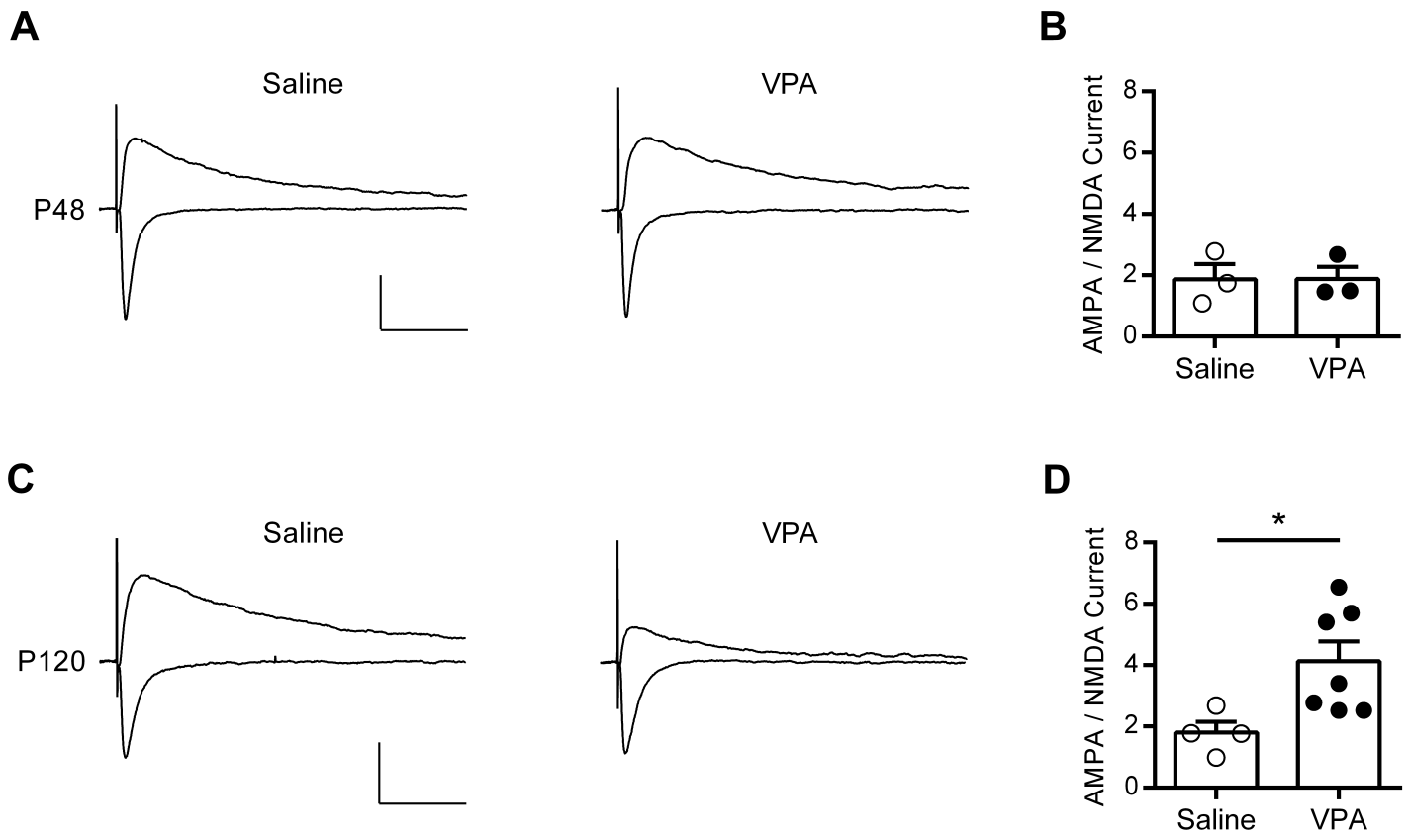


Figure 3.TIF

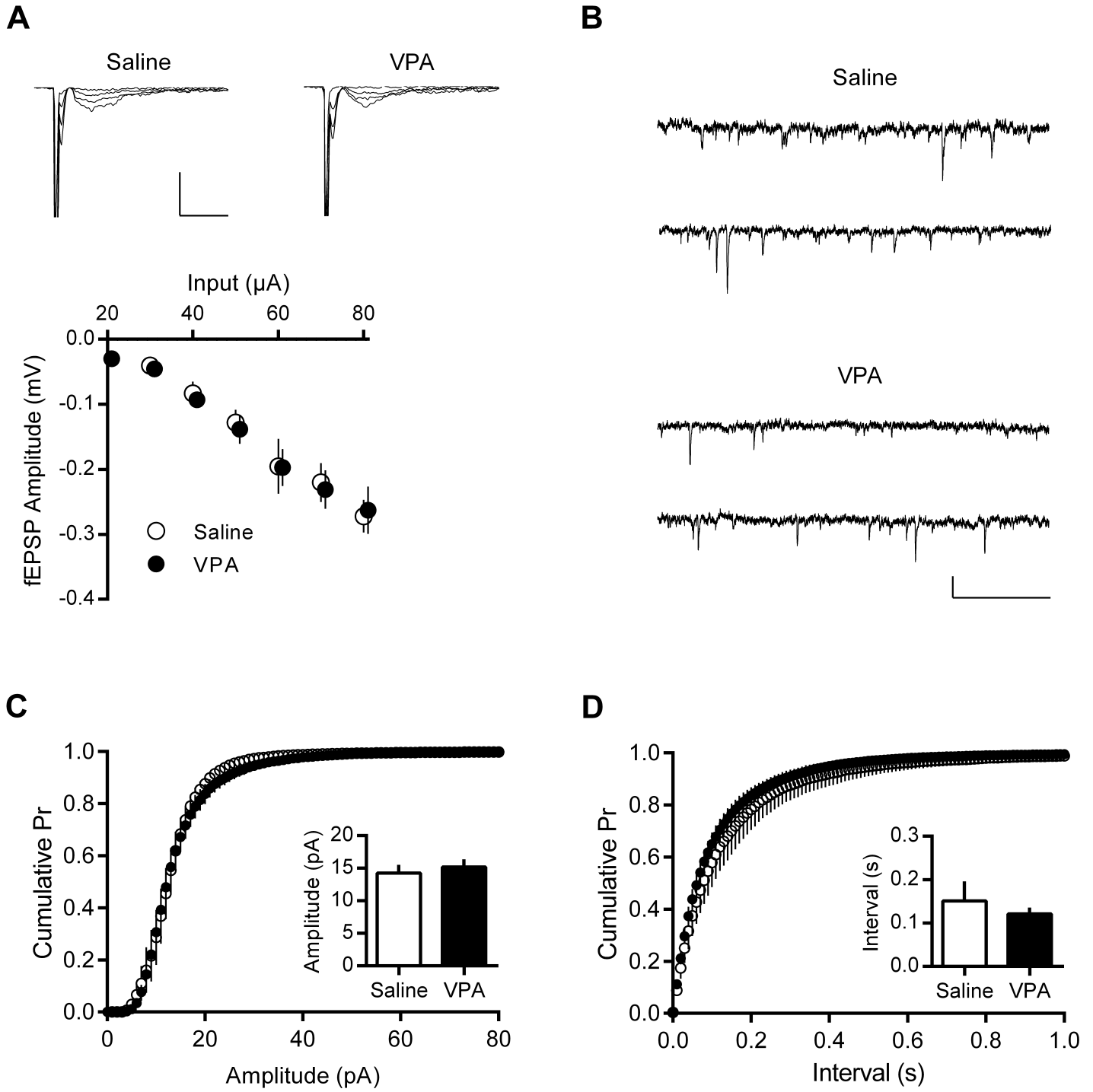
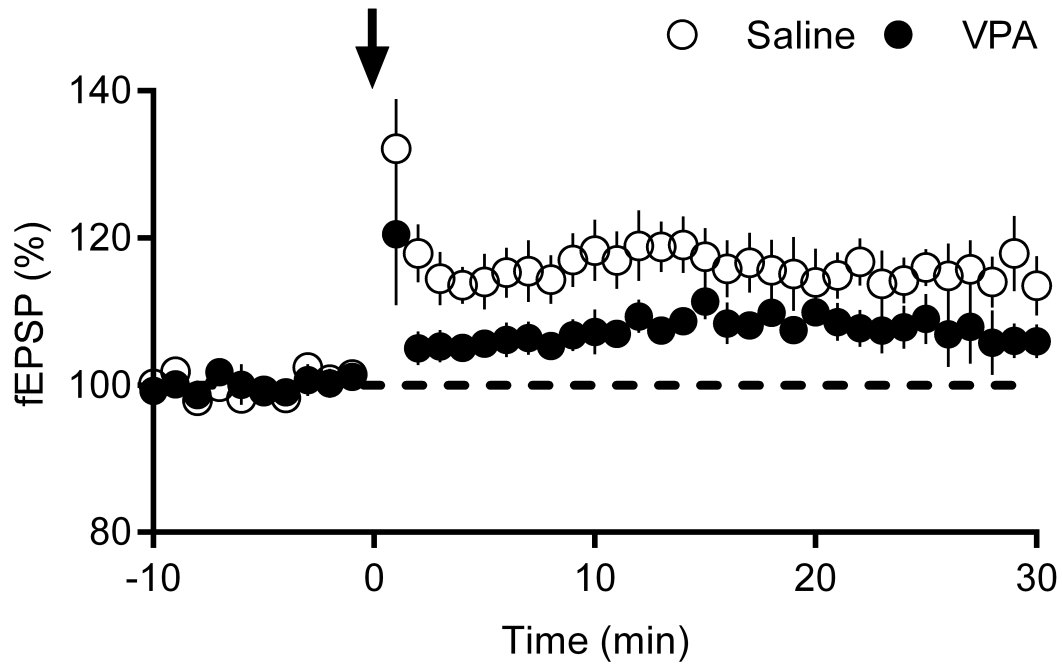
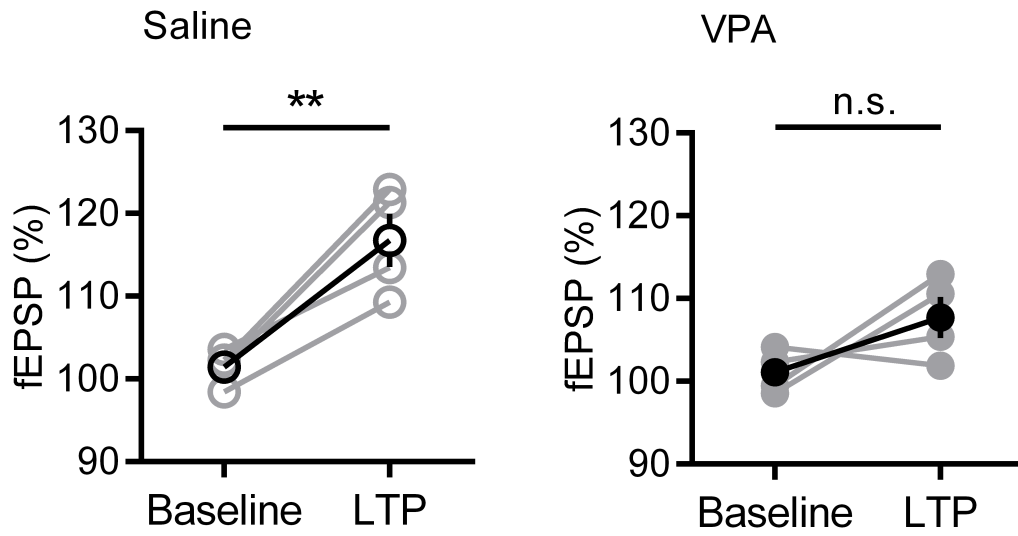


Figure 4.TIF

**A**



**B**



**C**

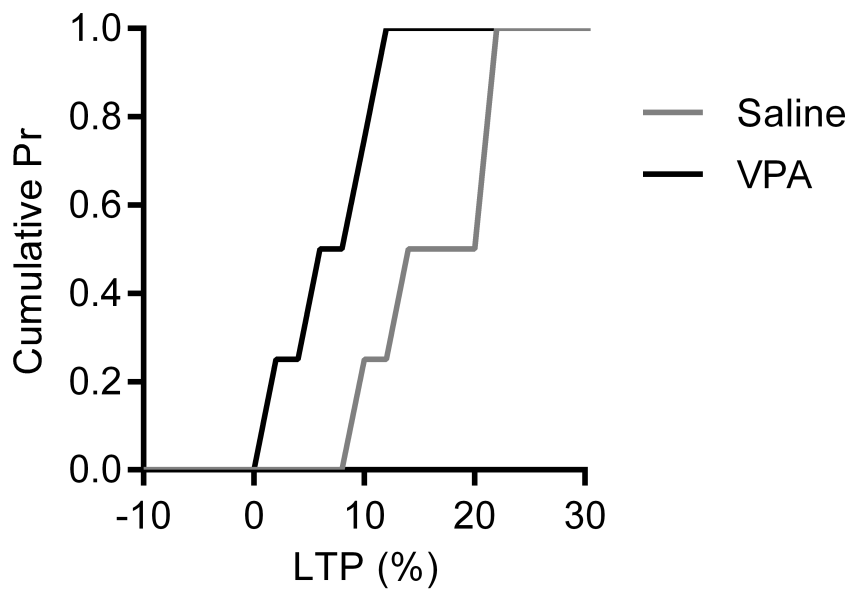
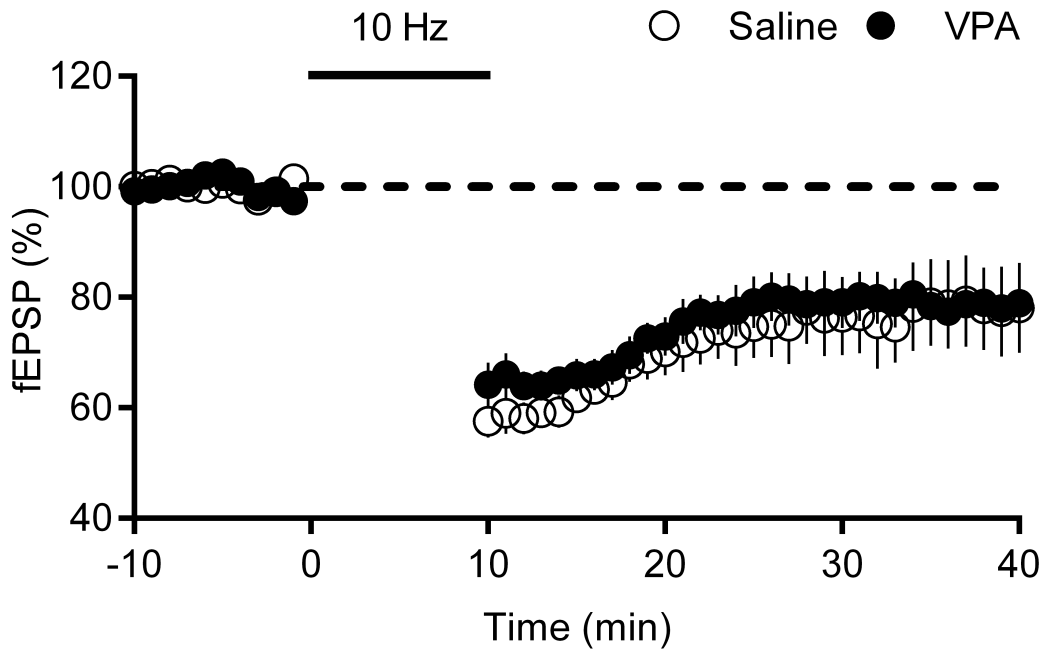
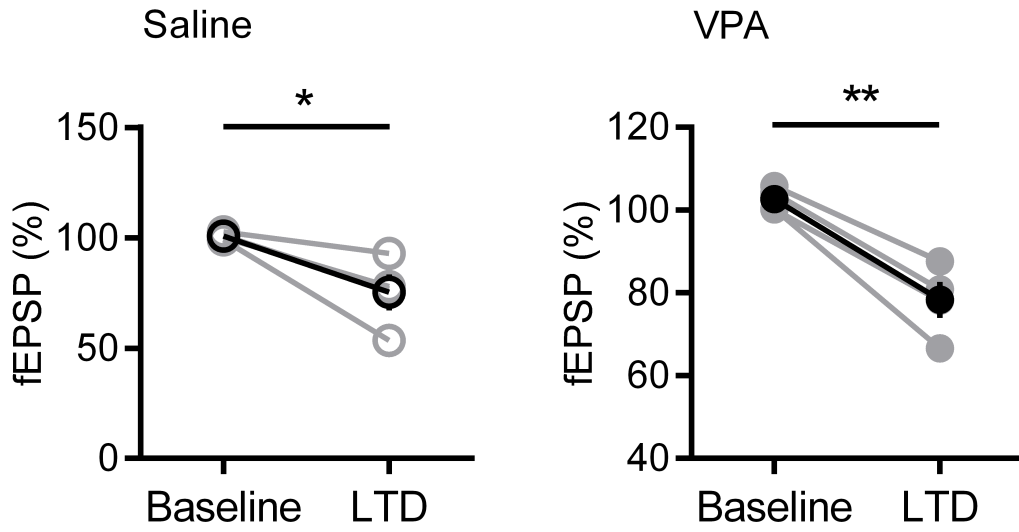


Figure 5.TIF

**A**



**B**



**C**

